

Arctic Amplification of marine heatwaves under global warming

Received: 5 September 2023

Accepted: 20 September 2024

Published online: 26 September 2024

 Check for updates

Yan He ^{1,2,3,8}, Qi Shu ^{1,2,3,8}, Qiang Wang ^{4,5} ✉, Zhenya Song ^{1,2,3},
Min Zhang ^{1,2,3}, Shizhu Wang^{1,2,3}, Lujun Zhang⁶, Haibo Bi⁷, Rongrong Pan^{1,2,3} &
Fangli Qiao ^{1,2,3} ✉

Marine heatwaves (MHWs) and total heat exposures (THEs), extreme warming events occurring across the global oceans, seriously threaten marine ecosystems and coastal communities as the climate warms. However, future changes in MHWs and THEs in the Arctic Ocean, where unique marine ecosystems are present, are still unclear. Here, based on the latest CMIP6 climate simulations, we find that both MHWs and THEs in the Arctic Ocean are anticipated to intensify in a warming climate, mainly due to Arctic sea ice decline and long-term warming trend, respectively. Particularly striking is the projected rise in MHW mean intensity during the 21st century in the Arctic Ocean, surpassing the global average by more than sevenfold under the CMIP6 SSP585 scenario. This phenomenon, coined the ‘Arctic MHW Amplification’, underscores an impending and disproportionately elevated threat to the Arctic marine life, necessitating targeted conservation and adaptive strategies.

Marine heatwaves (MHWs) are extreme ocean warming events that last for days to months^{1–4}. They pose severe threats to marine ecosystems and coastal communities^{5–7}. MHWs are widespread globally, including the Arctic Ocean located at the northernmost part of our planet^{8–13}. Remarkably, over the past 40 years, the mean intensity of MHWs in the Arctic marginal seas has been comparable with that observed in other regions of the world’s oceans⁹.

Global warming has been increasing seawater temperature, dramatically impacting the structure and geographic distribution of marine species and ecosystems^{5,14–16}. Confronted with thermal stress, some marine species have started to migrate poleward to cooler regions, including the Arctic Ocean^{17,18}. Despite this migration, the future evolution of MHWs in the Arctic Ocean and the threats these events pose to Arctic marine species remain unclear.

While some marine species may adapt to the gradual, long-term ocean warming induced by climate change, others may face challenges

in doing so^{14,19,20}. Therefore, it is crucial to differentiate between extreme warming events relative to a shifting ocean temperature baseline (known as MHWs) and those relative to a fixed historical temperature baseline (referred to as total heat exposures, THEs) when investigating their future evolution in a warming world^{21,22}. Providing insights into future changes in both MHWs and THEs can assist policymakers in assessing and proactively addressing the risks faced by various marine species.

In this study, we investigate historical (1985–2014) and future (2071–2100) MHWs and THEs in the Arctic Ocean using sea surface temperature (SST) and sea ice concentration (SIC) data from the Optimum Interaction Sea Surface Temperature v2.1 (OISST)²³, as well as historical simulations and future projections in the Coupled Model Intercomparison Project phase 6 (CMIP6)^{24,25} (Supplementary Table 1). The projections used in this study are based on four Shared Socio-economic Pathway (SSP) scenarios, including SSP126, SSP245, SSP370,

¹First Institute of Oceanography and Key Laboratory of Marine Science and Numerical Modeling, Ministry of Natural Resources, Qingdao, China. ²Laboratory for Regional Oceanography and Numerical Modeling, Qingdao Marine Science and Technology Center, Qingdao, China. ³Shandong Key Laboratory of Marine Science and Numerical Modeling, Qingdao, China. ⁴Alfred Wegener Institute, Helmholtz Centre for Polar and Marine Research (AWI), Bremerhaven, Germany. ⁵Key Laboratory of Ocean Observation and Forecasting and Key Laboratory of Ocean Circulation and Waves, Institute of Oceanology, Chinese Academy of Sciences, Qingdao, China. ⁶School of Atmospheric Sciences, Nanjing University, Nanjing, China. ⁷Key Laboratory of Marine Geology and Environment, Institute of Oceanology, Chinese Academy of Sciences, Qingdao, China. ⁸These authors contributed equally: Yan He, Qi Shu. ✉ e-mail: Qiang.Wang@awi.de; qiaofl@fio.org.cn

and SSP585, representing the low, medium, high, and high-end future forcing pathways^{25,26}, respectively. Here, the definitions of MHWs and THEs follow Amaya et al.²² (see “Methods”). We focus on four metrics to assess MHWs and THEs: mean intensity, annual total days, mean frequency, and mean duration. Mean intensity refers to the MHW/THE intensity averaged over MHW/THE events in a specific period. Annual total days represent the total number of days on which events occur each year. Mean frequency indicates the number of MHW/THE events per year averaged over a specific period. Mean duration indicates the duration of MHW/THE averaged over all events.

We reveal a much more prominent increase in MHW mean intensity in the Arctic in future warming climate when compared to the global ocean. Therefore, marine ecosystems in the Arctic may encounter increased threats from these extremes in the future, more so than their counterparts in lower-latitude oceans. We found that by the end of the 21st century, under the SSP585 warming scenario, the increase in MHW mean intensity in the Arctic is projected to be 7.6 times the global average, while the increase in THE mean intensity in the Arctic is expected to be 1.5 times the global average.

Results

MHWs and THEs in the past

The mean intensity of MHWs during the period of 1985–2014 derived from the OISST dataset is stronger in the Arctic marginal seas than in most ocean regions at mid and low latitudes, including coastal areas within economic zones (Fig. 1a, b). The multi-model mean (MMM) of CMIP6 successfully reproduces these observed features in MHW mean intensity in both the Arctic Ocean and lower latitude regions (Fig. 1e, f and Supplementary Fig. 1). The simulated magnitude of MHW mean intensity in the Arctic marginal seas closely aligns with observations, with typical values ranging from 2 to 3 °C (Fig. 1b, f).

The annual total days of MHWs in the OISST data set typically exceed 20 days in mid and low latitudes, as well as in most of the Nordic Seas. In contrast, the duration is shorter in the Arctic marginal seas, with the exception of the Barents Sea (Fig. 1c, d). This pattern of fewer annual total days of MHWs in the Arctic is well reproduced by the CMIP6 MMM (Fig. 1g, h). The models slightly overestimate the annual total days of MHWs in both the Arctic marginal seas and lower latitude

oceans (Fig. 1c, g and Supplementary Fig. 1), which is a typical model feature found before²⁷.

Due to extensive sea ice cover, MHWs were largely absent in the Arctic deep basin area in the historical period, as consistently shown by the OISST and CMIP6 MMM results (Fig. 1). Overall, the CMIP6 MMM reasonably simulates the main characteristics of past MHWs evident in the OISST dataset, despite some model biases in the magnitudes of the MHW intensity and annual total days. These biases echo those previously identified in CMIP5 simulations^{28,29}.

The spatial patterns of mean intensity and annual total days of THEs during 1985–2014, derived from both OISST and CMIP models, are quite similar to those of MHWs (Fig. 1 and Supplementary Fig. 2). Since THEs include contributions from long-term warming, their mean intensity is slightly larger than that of MHWs during the historical period.

MHWs and THEs in the future

MHWs and THEs over 2071–2100 under the SSP585 scenario^{25,26} of CMIP6 are analyzed to gain insights into how they will change in a future warming climate. Under the SSP585 warming scenario, MHWs with mean intensity surpassing 1 °C and THEs with mean intensity exceeding 2 °C are expected to become widespread across the majority of the global oceans over 2071–2100 (Fig. 2a, b, e, and f). Future MHWs are anticipated to have greater intensity in several regions, including the northwest Pacific and Atlantic oceans, the tropical Pacific Ocean, mid-latitude oceans in the Southern Hemisphere, and the Arctic Ocean (Fig. 2a). Similarly, future THEs are projected to be stronger in these regions compared to others (Fig. 2e). Notably, among the five global oceans, the Arctic Ocean is expected to experience the most intense MHWs and THEs in the future, with mean intensities of about 2 °C and 3 °C, respectively, in the period of 2071–2100 (Fig. 2a, b, e, and f). In the future, the intensity of MHWs and THEs in the Arctic Ocean will be larger than or at levels similar to hotspots of MHWs at mid and low latitudes (Supplementary Fig. 3).

Considering the global ocean, the most substantial increase in MHW mean intensity is projected to take place in the Arctic deep basin (Fig. 2c, d), while the MHW mean intensity in the Arctic marginal seas and in mid and low latitudes, where MHWs were prevalent in the past, is not anticipated to undergo marked changes in the future (Fig. 2c, d).

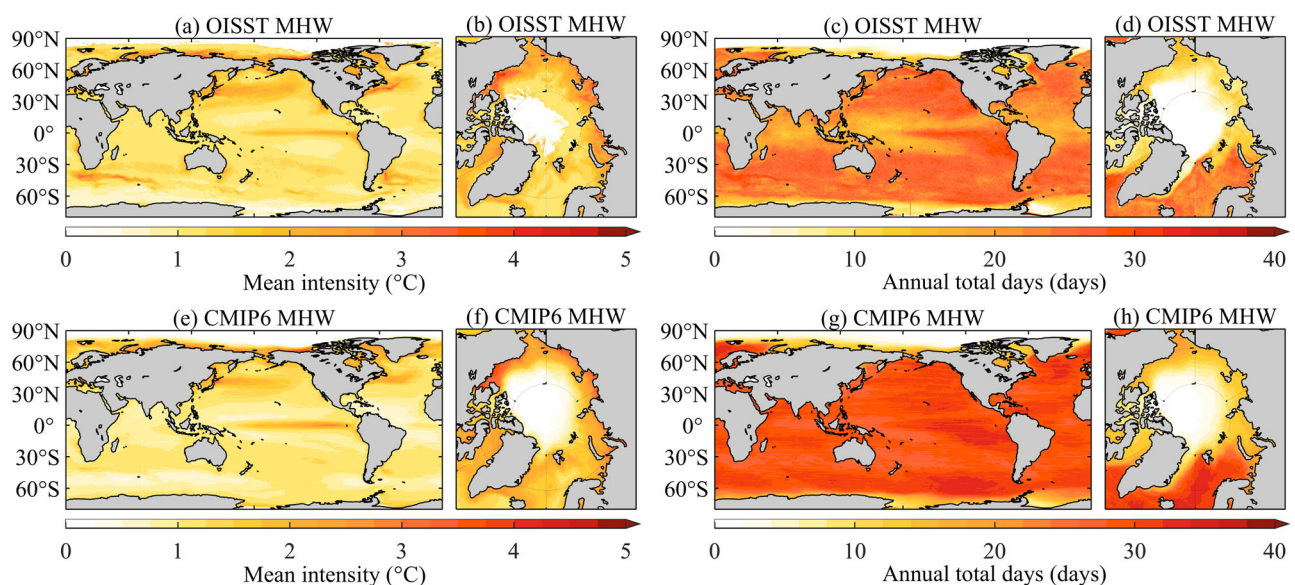


Fig. 1 | Mean intensity and annual total days of marine heatwaves (MHWs) during 1985–2014. a, b MHW mean intensity in the (a) global ocean and (b) Arctic Ocean derived from OISST. c, d The same as (a) and (b), but for MHW annual total

days. e–h The same as (a–d), but from the multi-model mean (MMM) of CMIP6 historical simulations.

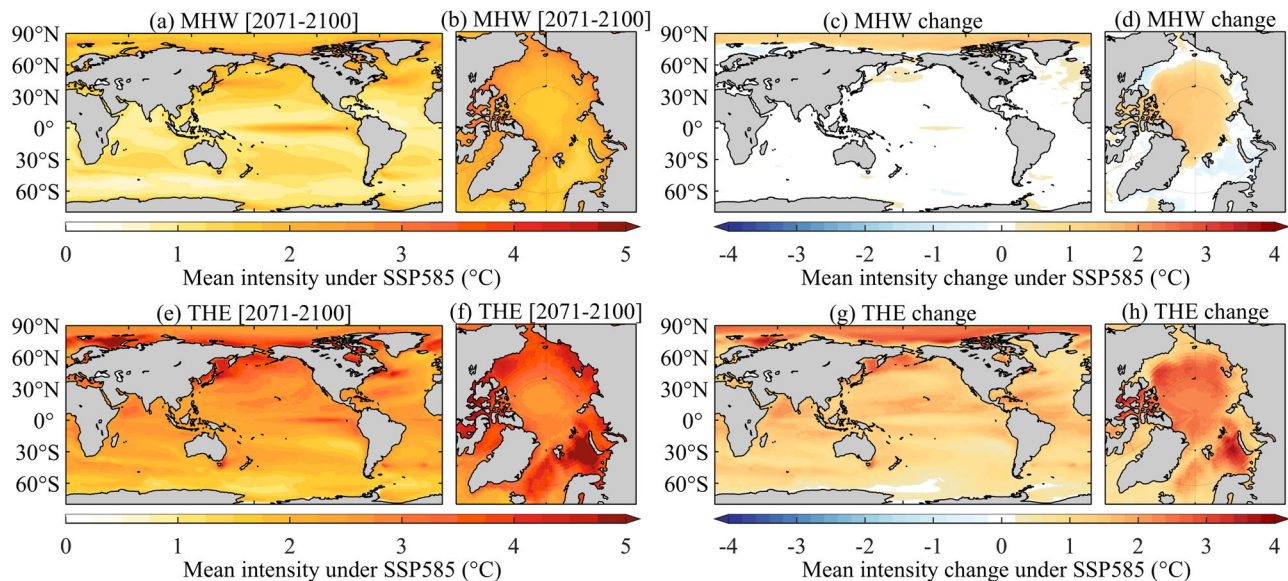


Fig. 2 | Mean intensity of marine heatwaves (MHWs) and total heat exposures (THEs) during 2071–2100 based on CMIP6 multi-model mean (MMM) under the SSP585 scenario. a, b MHW mean intensity in the (a) global ocean and (b) the

Arctic Ocean. **c, d** The changes in MHW mean intensity during 2071–2100 relative to 1985–2014 in the (c) global ocean and (d) the Arctic Ocean. **e–h** The same as (a)–(d), but for THE mean intensity.

In regions outside the Arctic Ocean, the future changes in MHW mean intensity in the period 2071–2100 relative to the period 1985–2014 will generally remain below 0.4 °C, including the coastal regions within economic zones, under the SSP585 scenario (Fig. 2c). This finding is in line with previous result based on dedicated numerical simulations²¹. Our results demonstrate that the MHW mean intensity in the deep basin area of the Arctic Ocean will exhibit a much more pronounced increase, by up to ~1.4 °C (Fig. 2d). This distinctive increase in MHW mean intensity across the central Arctic can be attributed to the notable reduction in sea ice coverage resulting from a warming climate. The MHW mean intensity over the central Arctic was quite weak in the past (Fig. 1b, f) because SST is close to the freezing point under sea ice cover. However, the anticipated shift toward a seasonally ice-free condition (Supplementary Fig. 4) will facilitate the development of MHWs in this region.

In the future warming climate, THEs will experience the most pronounced intensification within the Arctic Ocean (Fig. 2e–h). The increase in THE mean intensity under the SSP585 scenario is projected to reach ~3 °C in some areas of the Arctic Ocean, with the strongest increase expected in the Barents Sea, where it could amount to around 4 °C (Fig. 2h). The MHW mean intensity in the Barents Sea is projected not to increase in the future (Fig. 2d), so the increase in THE mean intensity in the Barents Sea is mainly due to the long-term warming trend, which can be attributed to both enhanced Atlantic Water heat inflow and reduced local heat loss to the atmosphere³⁰. In most of the Arctic shelf seas, the increase in THE mean intensity is also primarily driven by the long-term warming trend. For the central Arctic Ocean (approximately north of 75°N), our analysis indicates that the increase in MHW mean intensity accounts for about half of the increase in THE mean intensity, with the other half resulting from the direct effect of long-term warming.

The projected MHW annual total days during 2071–2100 resemble those of the historical period in terms of both their spatial pattern and magnitude across the global ocean, with the exception of the Arctic Ocean (Figs. 1g and 3a). The projected MHW annual total days in the Arctic Ocean (about 20 days) are shorter than those in the mid and low latitudes (about 30 days) (Fig. 3a, b). However, the most noteworthy increase in the annual total days of MHWs is expected within the Arctic deep basin (Fig. 3c, d), which corresponds to a substantial transition

from almost negligible MHW days in the past to approximately 20 days in the future (Figs. 1h and 3b).

Due to the long-term warming trend, future changes in the annual total days of THEs will markedly contrast with those of MHWs. Projections indicate that in the period 2071–2100, THE annual total days are expected to exceed 300 days across about 80% of the global ocean expanse (Fig. 3e), whereas, in the central Arctic, they are projected to hover around 200 days (Fig. 3f). Accordingly, the future increase in THE annual total days in the Arctic Ocean is expected to be more modest compared to the global average (Fig. 3g, h). This outcome can be attributed to the presence of winter sea ice cover in the period 2071–2100 (Supplementary Fig. 4), a factor that constrains THE occurrence of the cold season in the Arctic Ocean (Supplementary Fig. 5).

Tests for statistical significance reveal that most of the models surpass the 95% confidence level for the projected future changes in mean intensity and annual total days of MHWs and THEs in the Arctic Ocean. However, the projected future changes in mean intensity and annual total days of MHWs in the mid and low latitudes are insignificant in most of the models (Supplementary Fig. 6).

The mean frequency of MHWs and THEs in the Arctic Ocean is projected to markedly increase in the future warming climate (Supplementary Fig. 7). In contrast, a decrease or no remarkable change in frequency is anticipated for the majority of other ocean regions.

Main drivers of changes in MHW and THE mean intensity

Future increases in Arctic MHW intensity are more pronounced under scenarios with higher forcing pathways (Fig. 4a–d). Under all warming scenarios, future changes in the mean intensity of Arctic MHWs are significantly anti-correlated with future changes in Arctic sea ice area across the models during both the warm half-year (Fig. 4e–h) and cold half-year (Fig. 4j–m). This linear relationship suggests that the reduction in sea ice cover is a key driver for the projected increase in Arctic MHW intensity, consistent with findings on changes in Arctic MHW intensity over the past decades³¹. The extended periods of open ocean resulting from sea ice retreat allow for a greater accumulation of seasonal surface heat flux in the ocean, thereby triggering stronger MHWs³¹.

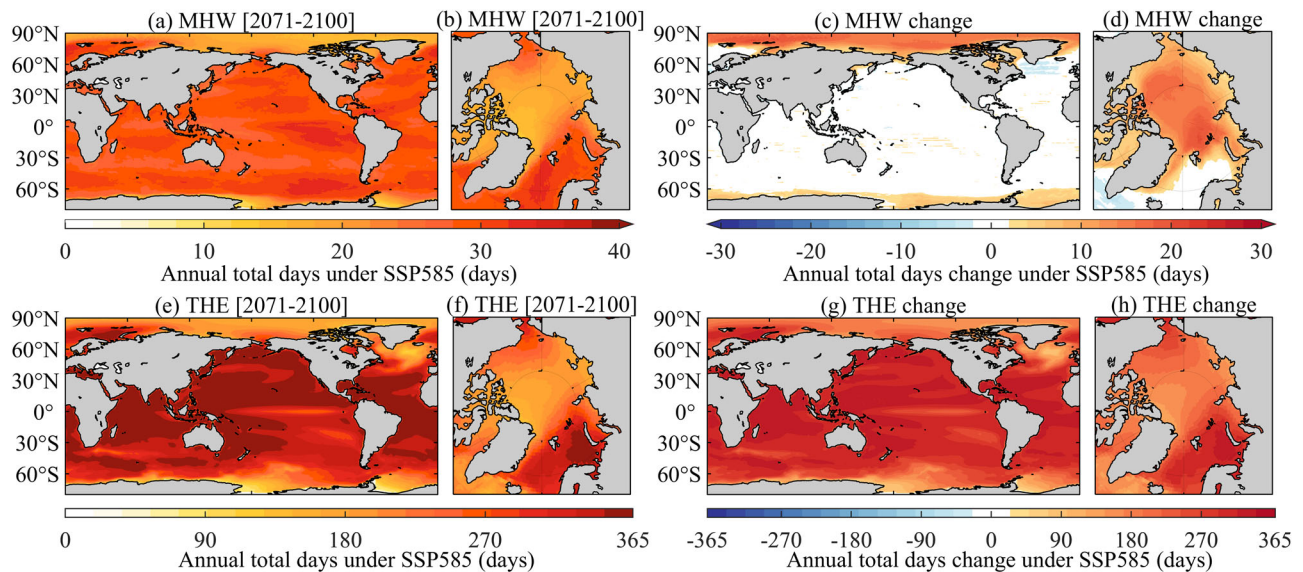


Fig. 3 | Annual total days of marine heatwaves (MHWs) and total heat exposures (THEs) during 2071–2100 based on CMIP6 multi-model mean (MMM) under the SSP585 scenario. a, b MHW annual total days during 2071–2100 in the

global ocean and the Arctic Ocean, respectively. **c, d** The changes of MHW annual total days during 2071–2100 relative to 1985–2014. **e–h** The same as (a–d), but for THE annual total days.

The correlation coefficient between future changes in Arctic MHW mean intensity and Arctic sea ice area is lower in the SSP585 scenario (Fig. 4h, m) than in other scenarios. This is because the Arctic is nearly free of sea ice during most months in the last few decades of the SSP585 scenario. In this situation, while the accumulation of surface heat flux in the ocean and consequently the MHW intensity can further increase with stronger atmospheric warming, the sea ice area cannot further decrease during months when it is already ice-free. This weakens the correlation between changes in MHW intensity and changes in sea ice area. However, if we focus only on the period from March to May when sea ice is still present at the end of the 21st century in the SSP585 scenario, the correlation coefficient between future changes in MHW mean intensity and Arctic sea ice area is higher (Fig. 4i) compared to longer seasonal considerations (Fig. 4h, m). This reinforces the dominant role of sea ice decline in driving changes in MHW intensity as long as the Arctic retains some sea ice. In the SSP585 warming scenario, when the Arctic Ocean becomes free of sea ice throughout the year in the far future (Supplementary Fig. 8), MHWs in the Arctic Ocean will enter a stage where the changes in mean intensity and annual total days are relatively small (Supplementary Fig. 9), similar to the situation in the mid and low latitudes in the 21st century (Figs. 2c and 3c).

The seasonality of changes in Arctic MHW intensity is similar across different warming scenarios (Fig. 4a–d), featuring two peaks: one in summer (June and July) and another in December. The summer peak is associated with the seasonal maximum in solar radiation and net ocean surface heat flux³² (Supplementary Fig. 10). Even with the same extent of sea ice retreat, greater seasonal solar radiation can lead to more heat absorption in the ocean. The December peak is mainly linked to the seasonal maximum in sea ice decline (Fig. 4a–d), which increases open water where MHWs can occur. Thus, the seasonality of future changes in MHW intensity is jointly determined by the seasonality of solar radiation and sea ice decline. The seasonality of future changes in the SST variance mirrors the seasonality of future changes in MHW intensity (Supplementary Fig. 11), indicating that SST variance is a good indicator of MHW intensity.

Future changes in the Arctic THE mean intensity is larger in summer (July–September) and smaller in winter (February–April) across all scenarios (Fig. 5a–d). This seasonality differs from that of changes in MHW mean intensity (Fig. 4a–d) and aligns more closely

with changes in SST (Fig. 5a–d), indicating that the long-term warming trend is the primary driver of increases in THE intensity. This conclusion is further supported by the strong correlation between future changes in THE mean intensity and future changes in SST across the models in all warming scenarios (Fig. 5e–h).

The projected Arctic Amplification of MHWs

Figures 2 and 3 show that future increases in both the MHW mean intensity and the annual total days in the Arctic Ocean considerably surpass the global ocean average under the SSP585 scenario. We term this phenomenon ‘Arctic MHW Amplification’.

To quantitatively compare the future changes in MHWs and THEs between the Arctic Ocean and the global ocean, the results for all the warming scenarios are presented in Fig. 6 and Supplementary Table 2.

The MMM difference of MHW mean intensity in the Arctic Ocean between 2071–2100 and 1985–2014 is 0.08, 0.18, 0.28, and 0.38 °C under SSP126, SSP245, SSP370, and SSP585, respectively. In contrast, the global ocean averages are 0.00, 0.02, 0.06, and 0.05 °C, respectively. Under the SSP585 scenario, the Arctic amplification factor of MHW mean intensity change is approximately 7.6. For THE mean intensity, the MMM difference is 0.16, 0.70, 1.17, and 1.82 °C under SSP126, SSP245, SSP370, and SSP585, respectively, while the global ocean averages are 0.14, 0.41, 0.75, and 1.21 °C, respectively. The Arctic amplification factor of THE mean intensity change is approximately 1.5 under the SSP585 scenario. Although THE amplification factor is relatively smaller, the changes in Arctic THE mean intensity are much larger than those of MHWs (Fig. 2). Therefore, it is crucial to emphasize the future changes of both Arctic MHWs and THEs.

For changes in the annual total days, Arctic amplification is found only for MHWs, not for THEs (Fig. 6b and d; Supplementary Table 2). Under the SSP585 scenario, the annual total days of MHWs are projected to increase by 9.45 days in the Arctic Ocean compared to 0.47 days in the global ocean. The THE annual total days are projected to increase by 223.58 days in the Arctic Ocean, less than the average (301.06 days) over the global ocean. In contrast, the increase in THE mean intensity in the Arctic is more pronounced than in the global ocean, as discussed above. This is because the mean intensity, per definition, is calculated by averaging over events. If there are no THE events in a period, this period does not contribute to lowering the calculated mean intensity.

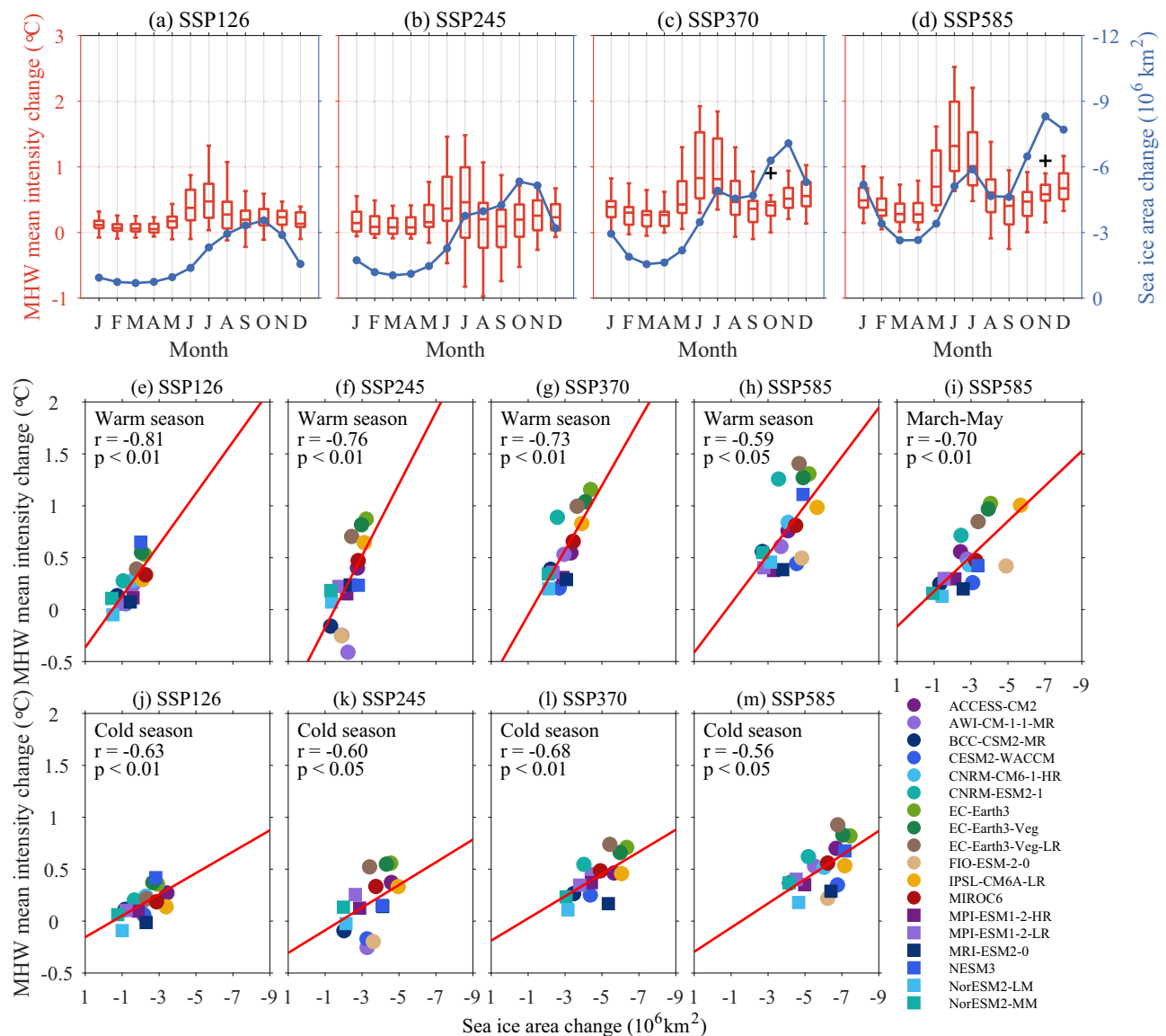


Fig. 4 | Relationship between changes in marine heatwave (MHW) mean intensity and sea ice area in the Arctic Ocean in different warming scenarios. a–d Monthly changes in MHW mean intensity (red box plots) and sea ice area (blue lines) in the Arctic Ocean. Correlations between MHW mean intensity changes and sea ice area changes across CMIP6 models during (e–h) warm season (March–August) and (j–m) cold season (September–February). **i** Correlation in the

period from March to May under the SSP585 scenario. In the box plots in (a–d), the marks inside the boxes indicate the median and the bottom and top edges of the boxes indicate the 25th percentile and 75th percentile, respectively. The red vertical lines extend to the most extreme data points not considered outliers. The black ‘+’ symbols denote outliers. The changes are the results of 2071–2100 relative to 1985–2014.

For both changes in the mean frequency and mean duration, Arctic amplification is found for MHWs under all four scenarios, but not for THEs (Supplementary Figs. 12 and 13). In the Arctic Ocean, the future increase in the mean frequency of MHWs correlates with the severity of warming scenarios. However, the mean duration of MHWs does not show a similar trend. Consequently, the frequency increase of MHWs is the primary contributor to the projected rise in the annual total days of Arctic MHWs. Conversely, for Arctic THEs, the future increase in their mean duration correlates with the severity of warming scenarios, while their frequency does not. Therefore, the increase in the mean duration of THEs is the main factor contributing to the future rise in the mean annual total days of Arctic THEs.

Discussion

Ocean temperature beneath sea ice in the Arctic is close to seawater freezing point which is primarily influenced by changes in sea surface salinity, exhibiting minor variations³³. Such temperature fluctuations

should not be considered when delineating MHW occurrences. A remarkable decline of Arctic sea ice in a warming climate enhances air-sea interaction, and the resulting strengthened atmospheric effects could induce temperature anomalies in open waters, consequently fostering increased MHW intensity, frequency, and duration in the Arctic⁹. Our findings indicate that sea ice decline is the primary driver for the future increase in Arctic MHW intensity, while the long-term ocean warming trend plays a major role in determining the magnitude of Arctic THE intensity. All the warming scenarios show an amplification of MHW and THE intensity in the Arctic Ocean compared to the global average.

Not only is the increase in the mean intensity of MHWs and THEs in the Arctic Ocean expected to surpass the global average but also the mean intensity itself in the Arctic Ocean is projected to be prominent by the end of the 21st century in a global context (Fig. 2). In the past, several notably severe warming events have been observed, causing ecological damages and potentially devastating consequences^{4,34}.

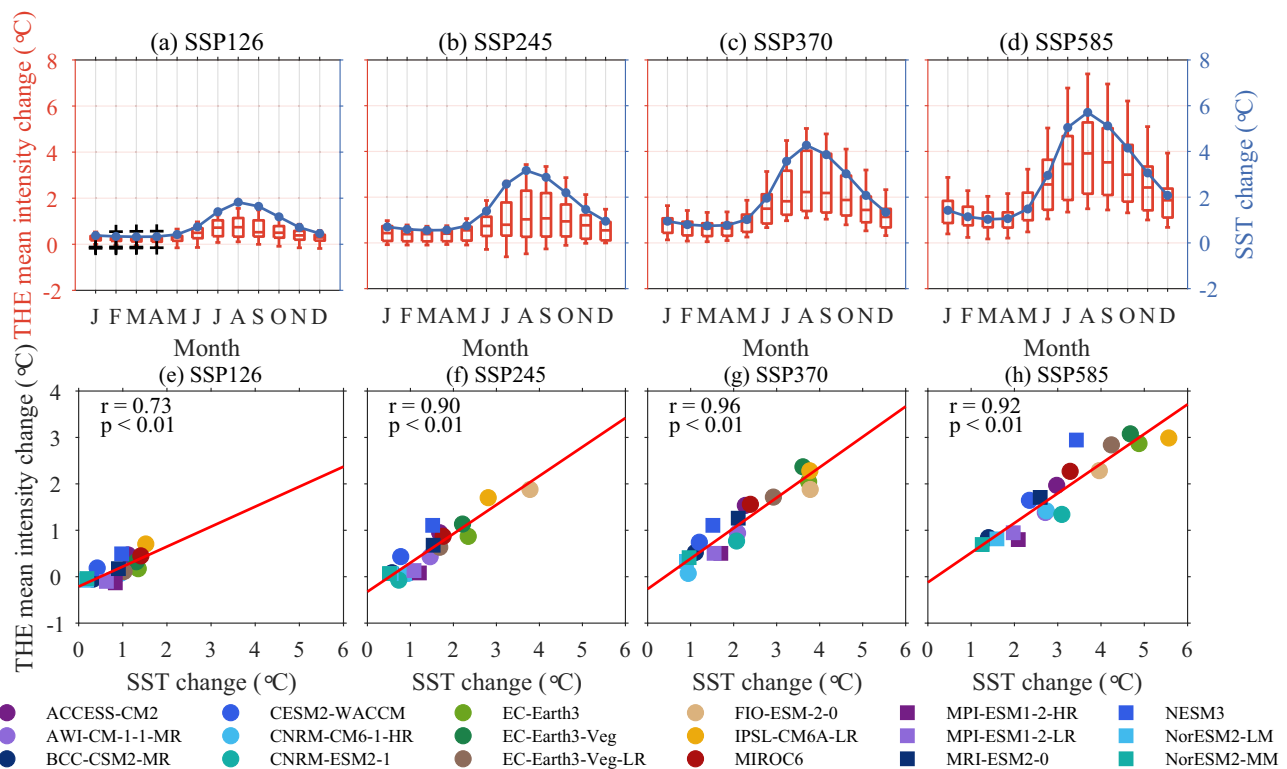


Fig. 5 | Relationship between changes in total heat exposure (THE) mean intensity and sea surface temperature (SST) in the Arctic Ocean in different warming scenarios. a–d Monthly changes in THE mean intensity (red box plots)

and sea surface temperature (blue lines). **e–h** Correlations between annual THE mean intensity changes and annual sea surface temperature changes across CMIP6 models. The changes are the results of 2071–2100 relative to 1985–2014.

Examples include the well-known 2014/15 ‘Blob’ in the northeast Pacific³⁵, the 1997/98 El Niño event in the tropical Pacific³⁶, and the warming event associated with the 2009 El Niño in the central south Pacific³⁷. Some western boundary current extension regions have also shown large temperature variability, which could bring both unanticipated challenges and opportunities to fisheries³⁸. These regions appear to have no notable changes in MHW mean intensity during the 21st century, and the future mean intensity of MHWs and THEs in the Arctic Ocean is anticipated to be stronger than or at the same level as these typical regions (Supplementary Fig. 3). The long-term warming trend in the Barents Sea is predicted to be the largest in the Arctic region³⁹, resulting in the highest THE mean intensity (Fig. 2e, f).

Moreover, the mean intensity of MHWs and THEs in the Arctic Ocean is projected to be notably greater compared to the polar seas in the Antarctic (Fig. 2), aligning with the amplified warming witnessed and predicted in both the atmosphere and the ocean in the Arctic region as a consequence of climate change^{39,40}.

An increase in MHW/THE intensity and annual total days can trigger extensive and enduring consequences for marine life⁴¹. MHWs and THEs have different impacts on marine life in low and mid latitudes²², and they might also have different impacts in the Arctic Ocean in the future. Climate warming is inducing structural change over large spatial scales at high latitudes, leading to a borealization of fish communities in the Arctic⁴². In the case of phytoplankton, even strongly increased temperatures can stimulate community productivity, whereas their response to different kinds of heatwaves varies⁴³. The Arctic MHW amplification, which could potentially exert even more substantial impacts on the ecosystems in the Arctic Ocean, warrants heightened attention. To attain a more holistic understanding of the threats that climate change poses to marine ecosystems and to guide policymaking, it is imperative to conduct quantitative assessments of the risks associated with the Arctic MHW amplification.

CMIP6 models demonstrate noticeable model spreads in the simulated MHWs and THEs (Figs. 4–6 and Supplementary Figs. 3, 5, 10–13). This is not surprising, given the range of simulated ocean temperatures in these models⁴⁴. Although using high model resolution could potentially improve the model representation of MHWs^{21,45}, it is important to note that model resolution is only one of the factors influencing the fidelity of Arctic Ocean temperature simulation⁴⁶. It is expected that systematically improved climate models in future CMIP simulations can provide more accurate projections of Arctic MHWs and THEs, offering more precise insights into their characteristics.

Methods

Datasets

OISST v2.1²³ used in this study is based on the Advanced Very High-Resolution Radiometer (AVHRR) infrared satellite SST data and observations from different platforms such as ships, buoys, and Argo floats. It has a spatial resolution of $0.25^\circ \times 0.25^\circ$, available at <https://www.ncei.noaa.gov/data/sea-surface-temperature-optimum-interpolation/v2.1/access/avhrr/>. It has been widely used in MHW studies^{8,9,13,37,45,47}. To determine whether a location is an open water, daily sea ice concentration (SIC) from OISST v2.1 is also used.

The model data are from the CMIP6 repository²⁴ (available at <https://esgf-index1.ceda.ac.uk/projects/cmip6-ceda/>). There are 18 CMIP6 models that have released daily SST and SIC datasets from their first realization of the historical experiment, 17 models under the SSP126, 16 models under SSP245, 15 models under SSP370, and 18 models under 585 scenarios²⁵ (Supplementary Table 1). Historical simulations for the period of 1985–2014 are used for comparison with OISST. The SSP126, SSP245, SSP370, and SSP585 scenarios represent low, medium, high, and high-end future forcing pathways with an effective radiative forcing of 2.6, 4.5, 7.0, and 8.5 W m^{-2} in 2100²⁵. The global mean surface air temperature anomalies for the period

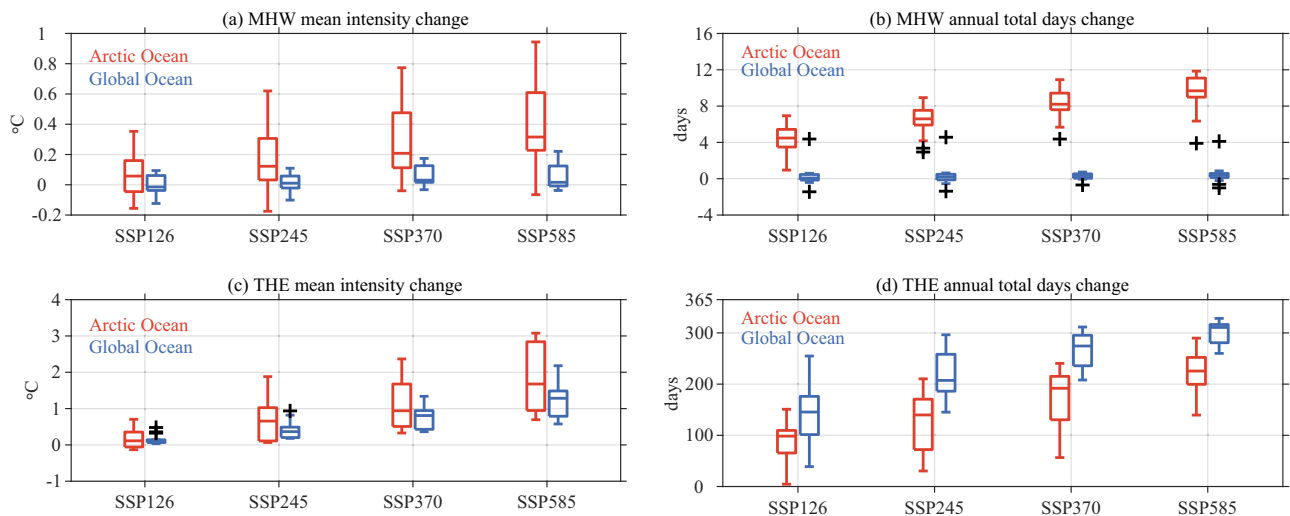


Fig. 6 | Comparison of future marine heatwave (MHW) and total heat exposure (THE) changes between the Arctic Ocean and the global ocean. a, c The mean intensity and **(b) and (d)** annual total days of MHWs and THEs averaged over the

Arctic Ocean and the global ocean in four warming scenarios. The red and blue box plots depict the results for the Arctic Ocean and the global ocean, respectively. The changes are the results of 2071–2100 relative to 1985–2014.

2081–2100 under these four scenarios are 1.23, 2.14, 3.16, and 3.99 °C relative to the period of 1995–2014⁴⁸.

Definitions and metrics of MHWs and THEs

MHWs refer to events of transient and extreme ocean warming relative to the climate condition of the period for which MHWs are considered. To distinguish the contributions from extreme ocean warming and long-term temperature trends, THE was proposed²². In this study, MHWs are calculated using detrended SST and a shifting baseline, while THEs are calculated using original SST and a fixed baseline (Supplementary Fig. 14). The baselines of MHWs for the historical and future periods are based on detrended SST in the historical and future periods, respectively. The baselines of THEs for the historical and future periods are the same, and both are based on the original SST in the historical period. So, the contributions from long-term warming are excluded in MHWs but included in THEs. That is, THEs represent the combination of long-term warming and MHWs. The analysis of MHWs and THEs, including the calculation of baselines, is performed for each model and each scenario separately before computing MMM results.

To detect MHWs and THEs, we followed the method of Hobday et al.² and used the toolbox from https://github.com/ZijieZhaoMMHW/m_mhw1.0 but with some modifications. MHWs/THEs are detected when ocean temperature is higher than the 90th percentile threshold, and the situation is sustained for at least five consecutive days with gaps of less than three days. The baseline and threshold for a certain day were calculated using all SST daily data within an 11-day window centered on this day from all years of the 30-year period²⁸. The obtained annual cycle of baseline and threshold values was then smoothed by applying a 31-day moving average²⁸. This method is effective in ice-free regions². For the Arctic Ocean, we have to pay attention to the impact of sea ice on SST in observations and model simulations. We notice that OISST v2.1 sets SST in ice-covered oceans ($SIC > 35\%$) to freezing points of seawater to reduce bias and random errors^{23,49}. We also used 35% SIC as a threshold for determining ice-free and ice-covered regions in this study. As the changes in the freezing point of seawater due to salinity changes are quite small, MHWs were considered to be absent under sea ice (where $SIC > 35\%$). If no MHW/THE event is detected at a location during the whole period, the metrics are set to 0 during MMM calculation.

In this study, we used several metrics to characterize MHWs and THEs, including mean intensity, annual total days, mean frequency,

and duration, which are defined following Hobday et al.² (Supplementary Fig. 14). MHW/THE mean intensity for each MHW/THE event is the mean temperature anomaly above the climatology (baseline) averaged over the event days (Supplementary Fig. 14). The mean intensity for a considered period is the average of the intensity for all the events in this period. Annual total days are defined as the total MHW/THE days per year. Mean frequency is defined as the annual number of occurrences of MHW/THE events averaged over the considered period. Duration is defined as the number of days between the start and end dates of an MHW/THE event (Supplementary Fig. 14), and mean duration indicates the average over all events during the considered period.

For seasonality analysis (Figs. 4, 5 and Supplementary Figs. 10, 11), MHW/THE monthly mean intensity cannot be calculated by averaging over events because an event may span calendar days of different calendar months. Therefore, we calculated the monthly mean intensity by averaging daily intensity on all event days in a calendar month.

The future changes are defined as the difference between the period of 2071–2100 and the period of 1985–2014 if not otherwise stated. The Arctic Ocean is defined as the ocean area north of 65°N.

Data availability

All the data used in this research are freely available to the public and can be downloaded through the links detailed in the Methods section. The data generated in this study have been deposited at <https://zenodo.org/records/13744458>.

Code availability

All codes used to produce the figures are available at <https://zenodo.org/records/13744458>.

References

- Pearce, A. et al. *The “Marine Heat Wave” off Western Australia during the Summer of 2010/11. Fisheries Research Report No. 222* (Department of Fisheries, 2011).
- Hobday, A. J. et al. A hierarchical approach to defining marine heatwaves. *Prog. Oceanogr.* **141**, 227–238 (2016).
- Oliver, E. C. J. et al. Longer and more frequent marine heatwaves over the past century. *Nat. Commun.* **9**, 1324 (2018).
- Oliver, E. C. J. et al. Marine heatwaves. *Annu. Rev. Mar. Sci.* **13**, 313–342 (2021).

5. Wernberg, T. et al. An extreme climatic event alters marine ecosystem structure in a global biodiversity hotspot. *Nat. Clim. Change* **3**, 78–88 (2013).
6. Smith, K. E. et al. Socioeconomic impacts of marine heatwaves: Global issues and opportunities. *Science* **374**, eabj3593 (2021).
7. Thoralf, F. et al. Unravelling seasonal trends in coastal marine heatwave metrics across global biogeographical realms. *Sci. Rep.* **12**, 7740 (2022).
8. Hu, S., Zhang, L. & Qian, S. Marine Heatwaves in the Arctic Region: Variation in Different Ice Covers. *Geophys. Res. Lett.* **47** (2020).
9. Huang, B. et al. Prolonged Marine Heatwaves in the Arctic: 1982–2020. *Geophys. Res. Lett.* **48**, <https://doi.org/10.1029/2021GL095590> (2021).
10. Frölicher, T. L., Fischer, E. M. & Gruber, N. Marine heatwaves under global warming. *Nature* **560**, 360–364 (2018).
11. Carvalho, K. S., Smith, T. E. & Wang, S. Bering Sea marine heatwaves: Patterns, trends and connections with the Arctic. *J. Hydrol.* **600**, 126462 (2021).
12. Mohamed, B., Nilsen, F. & Skogseth, R. Marine heatwaves characteristics in the Barents Sea based on high resolution satellite data (1982–2020). *Front. Mar. Sci.* **9**, <https://doi.org/10.3389/fmars.2022.821646> (2022).
13. Golubeva, E. et al. Marine heatwaves in Siberian Arctic Seas and adjacent region. *Remote Sens.* **13**, 4436 (2021).
14. Smale, D. A. et al. Marine heatwaves threaten global biodiversity and the provision of ecosystem services. *Nat. Clim. Change* **9**, 306–312 (2019).
15. Fuchs, H. L. et al. Wrong-way migrations of benthic species driven by ocean warming and larval transport. *Nat. Clim. Change* **10**, 1052–1056 (2020).
16. Xu, S. et al. Warming northward shifting southern limits of the iconic temperate seagrass (*Zostera marina*). *iScience* **25**, 104755 (2022).
17. Perry, A. L., Low, P. J., Ellis, J. R. & Reynolds, J. D. Climate change and distribution shifts in marine fishes. *Science* **308**, 1912–1915 (2005).
18. Sunday, J. M., Bates, A. E. & Dulvy, N. K. Thermal tolerance and the global redistribution of animals. *Nat. Clim. Change* **2**, 686–690 (2012).
19. Straub, S. C. et al. Resistance, extinction, and everything in between – The diverse responses of Seaweeds to Marine heatwaves. *Front. Mar. Sci.* **6**, 763 (2019).
20. Benthuisen, J. A., Oliver, E. C. J., Chen, K. & Wernberg, T. Editorial: Advances in understanding Marine heatwaves and their impacts. *Front. Mar. Sci.* **7**, 147 (2020).
21. Guo, X. et al. Threat by marine heatwaves to adaptive large marine ecosystems in an eddy-resolving model. *Nat. Clim. Change* **12**, 179–186 (2022).
22. Amaya, D. J. et al. Marine heatwaves need clear definitions so coastal communities can adapt. *Nature* **616**, 29–32 (2023).
23. Huang, B. et al. Improvements of the Daily Optimum Interpolation Sea Surface Temperature (DOISST) version 2.1. *J. Clim.* **34**, 2923–2939 (2021).
24. Eyring, V. et al. Overview of the Coupled Model Intercomparison Project Phase 6 (CMIP6) experimental design and organization. *Geosci. Model Dev.* **9**, <https://doi.org/10.5194/gmd-9-1937-2016> (2016).
25. O'Neill, B. C. et al. The Scenario Model Intercomparison Project (ScenarioMIP) for CMIP6. *Geosci. Model Dev.* **9**, 3461–3482 (2016).
26. Riahi, K. et al. The shared socioeconomic pathways and their energy, land use, and greenhouse gas emissions implications: An overview. *Glob. Environ. Change* **42**, 153–168 (2017).
27. Qiu, Z., Qiao, F., Jang, C., Zhang, L. & Song, Z. Evaluation and projection of global marine heatwaves based on CMIP6 models. *Deep Sea Res. Part II Topical Stud. Oceanogr.* **194**, 104998 (2021).
28. Oliver, E. C. J. et al. Projected Marine heatwaves in the 21st century and the potential for ecological impact. *Front. Mar. Sci.* **6**, 734 (2019).
29. Plecha, S. M., Soares, P. M. M., Silva, S. M. & Narvaez, W. D. C. On the uncertainty of future projections of Marine Heatwave events in the North Atlantic Ocean. *Clim. Dyn.* **56**, 7–8 (2021).
30. Shu, Q., Wang, Q., Song, Z. & Qiao, F. The poleward enhanced Arctic Ocean cooling machine in a warming climate. *Nat. Commun.* **12**, 2966 (2021).
31. Barkhordarian, A. et al. Arctic marine heatwaves forced by greenhouse gases and triggered by abrupt sea-ice melt. *Commun. Earth Environ.* **5**, 57 (2024).
32. Han, J., Park, H. & Chung, E. Projections of central Arctic summer sea surface temperatures in CMIP6. *Environ. Res. Lett.* **18**, 124047 (2023).
33. Carton, J. A., Ding, Y. & Arrigo, K. R. The seasonal cycle of the Arctic Ocean under climate change. *Geophys. Res. Lett.* **42**, 7681–7686 (2015).
34. Holbrook, N. J. et al. Keeping pace with marine heatwaves. *Nat. Rev. Earth Environ.* **1**, 482–293 (2020).
35. Bond, N. A., Cronin, M. F., Freeland, H. & Mantua, N. Causes and impacts of the 2014 warm anomaly in the NE Pacific. *Geophys. Res. Lett.* **42**, 3414–3420 (2015).
36. McPhaden, M. J. Genesis and evolution of the 1997–98 El Niño. *Science* **283**, 950–954 (1999).
37. Holbrook, N. J. et al. A global assessment of marine heatwaves and their drivers. *Nat. Commun.* **10**, 2624 (2019).
38. Mills, K. E. et al. Fisheries management in a changing climate lessons from the 2012 Ocean heat wave in the Northwest Atlantic. *Oceanography* **26**, 191–195 (2013).
39. Shu, Q. et al. Arctic Ocean amplification in a warming climate in CMIP6 models. *Sci. Adv.* **8**, eabn9755 (2022).
40. Graversen, R. G. et al. Vertical structure of recent Arctic warming. *Nature* **451**, 53–56 (2008).
41. Wernberg, T. et al. Climate-driven regime shift of a temperate marine ecosystem. *Science* **353**, 169–172 (2016).
42. Fossheim, M. et al. Recent warming leads to a rapid borealization of fish communities in the Arctic. *Nat. Clim. Change* **5**, 673–677 (2015).
43. Wolf et al. Heatwave responses of Arctic phytoplankton communities are driven by combined impacts of warming and cooling. *Sci. Adv.* **10**, ead15904 (2024).
44. Khosravi, N. et al. The Arctic Ocean in CMIP6 models: Biases and projected changes in temperature and salinity. *Earth's Future* **10**, e2021EF002282 (2022).
45. Bian, C. et al. Oceanic mesoscale eddies as crucial drivers of global marine heatwaves. *Nat. Commun.* **14**, 2970 (2023).
46. Wang, Q. et al. Impact of increased resolution on Arctic Ocean simulations in Ocean Model Intercomparison Project phase 2 (OMIP-2). *Geosci. Model Dev.* **17**, 347–379 (2023).
47. Jacox, M. G. et al. Global seasonal forecasts of marine heatwaves. *Nature* **604**, 486–490 (2022).
48. Tebaldi, C. et al. Climate model projections from the Scenario Model Intercomparison Project (ScenarioMIP) of CMIP6. *Earth Syst. Dyn.* **12**, 253–293 (2021).
49. Banzon, V., Smith, T. M., Steele, M., Huang, B. & Zhang, H. M. Improved estimation of proxy sea surface temperature in the Arctic. *J. Atmos. Ocean. Technol.* **37**, 341–349 (2020).

Acknowledgements

This work was supported by the National Natural Science Foundation of China (Grant Nos. 41821004 and 42276253) and the National Key Research and Development Program of China (Grant No. 2023YFF0804600). Q.S. was supported by the Shandong Provincial Natural Science Foundation (Grant No. ZR2022JQ17) and the Taishan Scholars Program (Grant No. tsqn202211264).

Author contributions

Q.W. and F.Q. conceived the study. Y.H. and Q.S. performed data analysis. Y.H., Q.S., and Q.W. wrote the initial manuscript. Y.H., Q.S., Q.W., Z.S., M.Z., S.W., L.Z., H.B., R.P., and F.Q. contributed to interpreting results, discussion of the associated dynamics, and improvement of this paper.

Competing interests

The authors declare no competing interests.

Additional information

Supplementary information The online version contains supplementary material available at <https://doi.org/10.1038/s41467-024-52760-1>.

Correspondence and requests for materials should be addressed to Qiang Wang or Fangli Qiao.

Peer review information *Nature Communications* thanks the anonymous reviewers for their contribution to the peer review of this work. A peer review file is available.

Reprints and permissions information is available at <http://www.nature.com/reprints>

Publisher's note Springer Nature remains neutral with regard to jurisdictional claims in published maps and institutional affiliations.

Open Access This article is licensed under a Creative Commons Attribution-NonCommercial-NoDerivatives 4.0 International License, which permits any non-commercial use, sharing, distribution and reproduction in any medium or format, as long as you give appropriate credit to the original author(s) and the source, provide a link to the Creative Commons licence, and indicate if you modified the licensed material. You do not have permission under this licence to share adapted material derived from this article or parts of it. The images or other third party material in this article are included in the article's Creative Commons licence, unless indicated otherwise in a credit line to the material. If material is not included in the article's Creative Commons licence and your intended use is not permitted by statutory regulation or exceeds the permitted use, you will need to obtain permission directly from the copyright holder. To view a copy of this licence, visit <http://creativecommons.org/licenses/by-nc-nd/4.0/>.

© The Author(s) 2024